Sensitivity Response of Total Focusing Method (TFM) for Weld Inspection Versus Other Techniques

Jeremy CARIGNAN [1] Marie-Pierre DESPAUX [2], François LACHANCE [3], Philippe RIOUX [4]

[1] Centre de métallurgie du Québec, Trois-Rivières, Québec, Canada

[1] Phone: (819) 376-8707 x5026; courriel: jeremy.carignan@cegeptr.qc.ca

[2 3 4] Sonatest, Quebec City, Québec, Canada

[2 3 4] Phones: (418) 686-6222; e-mail: despauxm@sonatest.com, lachancef@sonatest.com, riouxp@sonatest.com

Abstract

Total Focusing Method (TFM) is an ultrasonic-based technique enhanced with the post-processing algorithm. TFM generates an image virtually focused at every pixel with increased probability of detection for certain applications specific scenarios where enhanced defect sizing and characterisation is critical. Although TFM is greatly promoted, there are some concerns, especially for weld inspection. This article evaluates the amplitude variation towards specific flaw orientation and compares it with other techniques, such as phased array ultrasonic testing (PAUT) and radiographic testing (RT).

Keywords: NDT (non-destructive testing or evaluation), Weld Inspection, Total Focusing Method (TFM), Full Matrix Capture (FMC), Phased Array Ultrasonic Testing (PAUT), Radiographic Testing (RT).

1 Introduction

This study was inspired by the doctoral thesis of Madame Kombossé Sy from the Université Paris-Saclay [1]. In her studies, Ms Kombossé claims that some defect orientations would respond better to certain propagation modes while using the Total Focusing Method (TFM) algorithm. In her thesis, Ms Kombossé conducts her conclusion mostly on CIVA simulations based on artificial alike flaws. The objective of this case study is to validate this claim with a real weld sample, having real flaws alike as well as adding the phased array ultrasonic testing (PAUT) sensitivity comparison. Other techniques such as radiography and metallography have been used along as a complementary tool for further verification.

2 FMC/TFM Glossary

2.1 Full Matrix Capture

Full matrix capture (FMC) is an acquisition technique where each element of a phased-array transducer is individually pulsed and the echoes are received from each individual element, including the transmitter. It generates a matrix signal with raw A-scan information. In fact, the FMC collects many data at once. This data can be further analysed in the post-acquisition phase.

2.2 Total Focusing Method

Total focusing method (TFM) is the post-acquisition phase of an FMC inspection. It processes the raw A-scan signals with the help of algorithms to display the FMC data in a clear visual format [1]. Every computed pixel of a TFM image is the summation of all the signals passing through this particular pixel.

2.3 Propagation Modes

The TFM uses different wave propagation modes based on the flaw orientation, as seen in Figure 1. Some propagation modes are suitable depending on the flaw orientation.

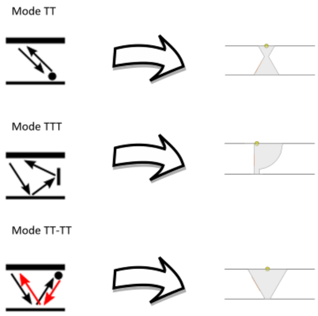

Figure 1 - Recommended propagation mode depending on the flaw orientation in the weld

3 Methodology

A 19 mm thick carbon steel plate with an unknown weld geometry and unknown flaws are used for the inspection, as per Figure 2. The groove angle was approximated at 45º and for the purpose of this study, PAUT, FMC/TFM, radiography Testing (RT) and metallography processes will be used to detect the flaws.

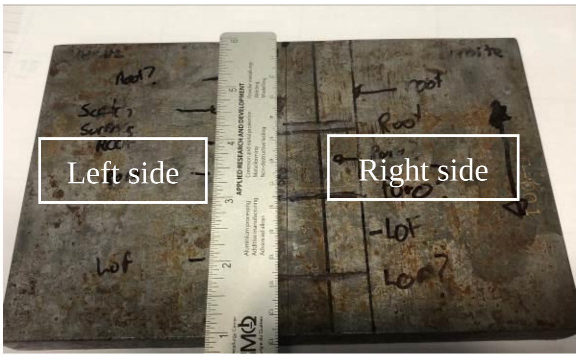

Figure 2 – The inspected plate prior to destructive testing

3.1 Ultrasonic Methodology

The Sonatest VEO+ platform along with 5 MHz DAAH transducer (model D1A) was used to record the PAUT and FMC data. Velocity, wedge delay, sensitivity and TCG calibrations were performed in order to compare the amplitude difference between flaws. Furthermore, the PAUT and TFM acquisitions were performed at the same time with the same probes and PA unit. Hence, the only parameters that could influence the results were the flaw orientation and the amplitude reference levels.

3.2 Radiography Methodology

The initial exposures were carried out with analogue film and then adapted to other techniques. The three expositions (0, +45º and -45º) were performed for each technique to detect possible lack of fusion and to determine the discontinuity heights.

Table 1 - Analogue film parameters

Distance between the source of the film	914 mm
Energy	200 kV
Exposure	2700 mA•sec.
Film brand	Carestream Industrex MX125
Pb intensity screen	0.127 mm front and 0.254 mm back
Filtration added to the X-ray tube	None
Optical density	2.5

3.2.1 Computed Radiography Technique

Both the exposure and the energy level were kept the same compared to the analogue technique. However, the laser power and the photomultiplier (PMT) were adjusted in combination with a Carestream Flex HR plate. A copper screen was used between the back of the imaging plate and the intensifying screen to prevent any lead fluorescence that could degrade the signal-to-noise ratio (SNR) of the image. A SNR of 130 was attained in the weld area and a contrast-to-noise ratio (CNR) of more of 3.5 was obtained.

3.2.2 Digital Radiography Technique

The main objective was to achieve similar SNR and CNR values to those of the computed radiography (CR) exposures. A 14-bit RayzorX Pro digital detector array (DDA) from Vidisco was used. The energy was raised to 240 kV, additional filtration was added to the tube window and the DDA was put farther away from the floor to reduce the scattered radiation and reduce the noise to achieve the acceptable SNR and CNR.

3.3 Metallography Methodology

Metallography were made regarding certain defects found with PAUT and TFM. All samples were grinded with silicon carbine paper submerged in water from 180 to 1200 grits [2]. Later different polycrystalline diamond solutions were used for polishing. The final step was accomplished with 0.05 μm colloidal alumina [2]. The etching reagent, Nital 2%, was applied for approximately 15 seconds [2].

4 Results

4.1 Radiography, Ultrasound & Metallography Overview of the Sample

Figure 3 illustrates the results obtained from all the non-destructive techniques. The first image is an End View: i.e. a cross section view from the left side of the weld. The second one is a radiography film of the same weld, and the other End View is from the right side of the weld.

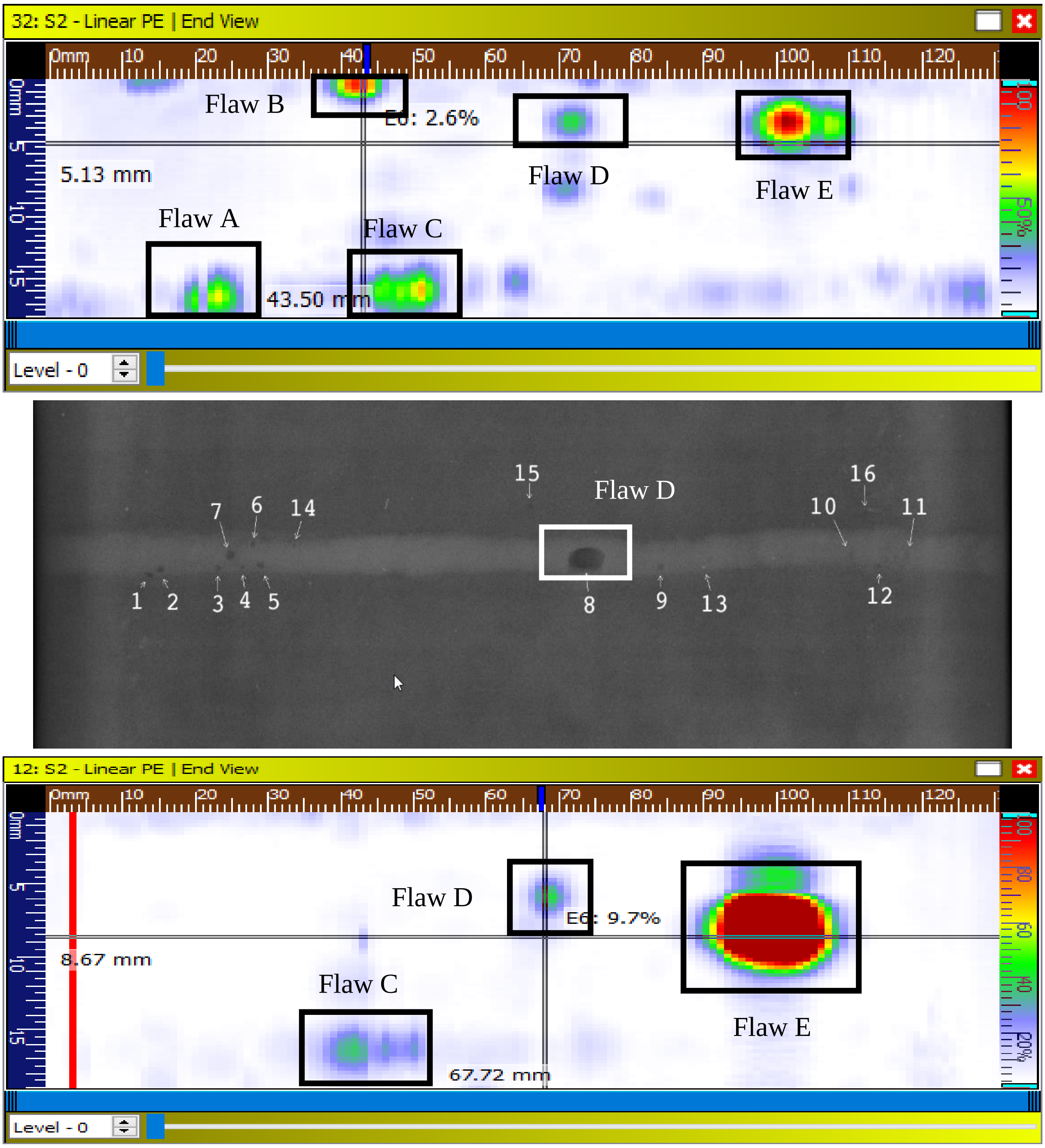

Figure 3 – The juxtaposed figures provide a better overview of the discontinuities in the plate.

In general RT is more sensitive in comparison to PAUT when dealing with volumetric flaws such as porosity and inclusion. On the other hand, PAUT is more sensitive for planar flaws such as crack or lack of fusion. All the numbers written on the X-ray except #13, which is an inclusion, correspond to porosities. Meanwhile the PAUT detected planar discontinuities were not visible in radiography. The same flaws have been detected by both PA and FMC/TFM test methods.

Metallography, since it is a destructive test, can eliminate any doubts about the defect's nature. The lack of fusion (flaw A) is visible at the root level, as seen in Figure 4, where there is a drastic change in microstructure at this location. Moreover, some porosities are visible at the root. Figure 5 shows two cracks landing to the surface. The big black spot, of the Figure 6, located in the middle of the weld, is the only porosity detected by PAUT and TFM. The fine line at the bevel of the Figure 7 is a lack of fusion.

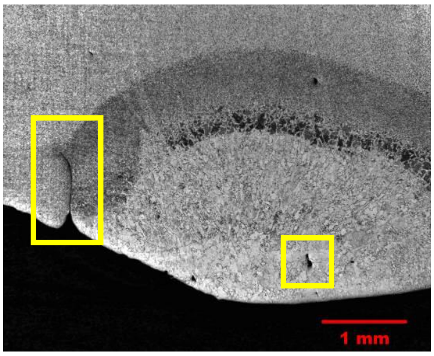

Figure 4 – Metallography of the flaw A

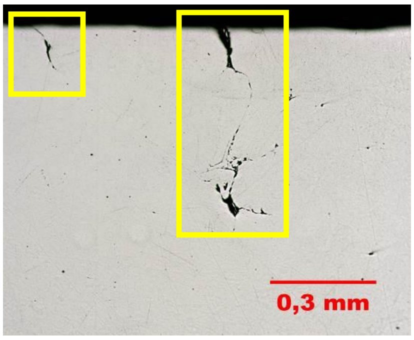

Figure 5 – Metallography of the flaw B

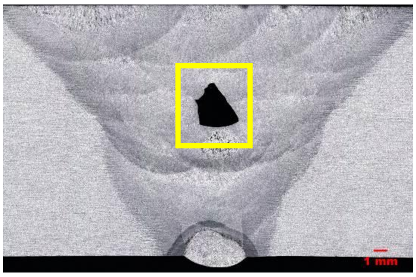

Figure 6 – Metallography of the flaw D

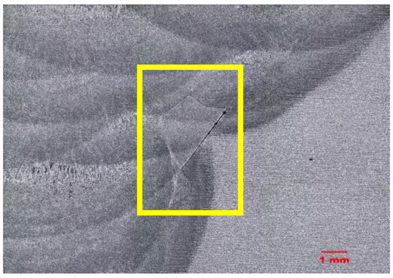

Figure 7 – Metallography of the flaw E

4.2 PAUT & TFM Differences

The major advantages of the TFM images compared to the PAUT scan are the improved resolution and the fact that the acoustic energy is virtually focused everywhere inside the weld volume. Such benefits are only achieved when the image is processed using the proper propagation mode towards the flaw orientation. Section 4.3 emphasises the importance of selecting the appropriate propagation mode according to the expected flaw orientation. Table 2 illustrates, in more details, the defect detected by ultrasonic techniques. For TFM pictures, only best propagation modes are chosen, the location and the acoustic signature of the flaws are included in this table.

Table 2 – PAUT and TFM defect characterisation comparison

Flaw A		**Flaw B**	
PAUT	TFM	PAUT	TFM
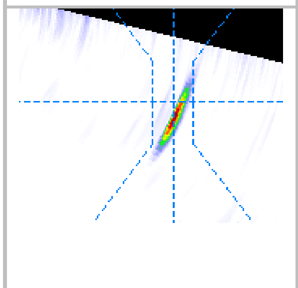	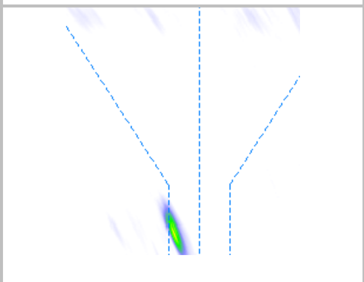	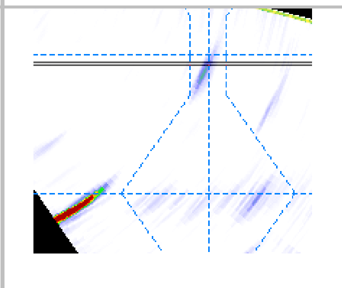	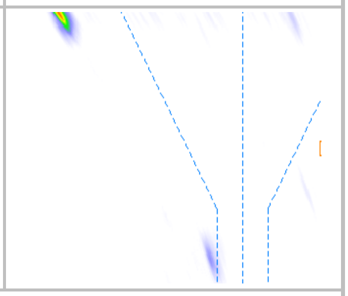
Type of defect: Lack of fusion near the root		Type of defect: Crack	
Location: 20 mm based on the scan axis		Location: 42 mm based on the scan axis	
Acoustic information: Strong amplitude response at the bevel or at the root		Acoustic information: Planar defect with distinguished amplitude response	
Is it detectable with: ☐RT ☒Metallography (see Figure 4)		Is it detectable with: ☐RT ☒Metallography (see Figure 5)	

Flaw C		Flaw D	
PAUT	TFM	PAUT	TFM
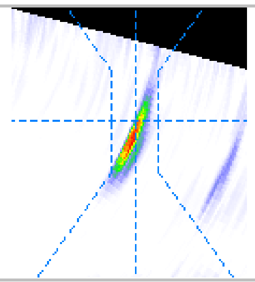	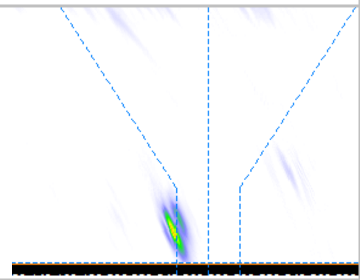	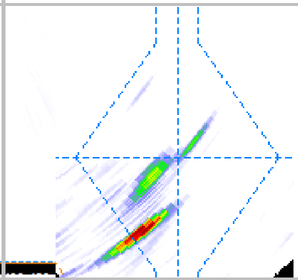	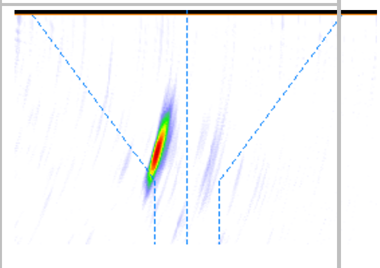
Type of defect: Root indication		Type of defect: Porosity	
Location: 50 mm based on the scan axis		Location: 70 mm based on the scan axis	
Acoustic information: Signal at the root		Acoustic information: Echo cluster in the weld volume	
Is it detectable with: ☐RT ☒Metallography		Is it detectable with: ☒RT (see Figure 3, #8 of the radiography film) ☒Metallography (see Figure 6)	

Flaw E	
PAUT	TFM
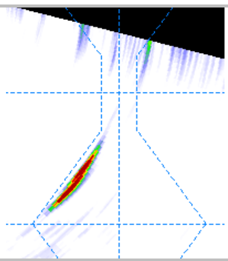	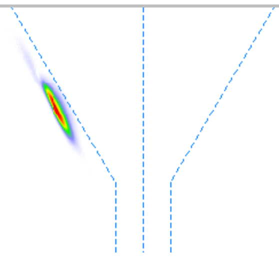
Type of defect: Lack of fusion	
Location: 100 mm based on the scan axis	
Acoustic information: Strong amplitude response at the bevel	
Is it detectable with: ☐RT ☒Metallography (see Figure 7)	

Apart from the improvement in resolution, the physical representation of the amplitude is the main difference between PAUT and TFM. The image reconstruction algorithm of the TFM makes the amplitude comparison difficult. However, both amplitude representations are still meant to represent the sound energy level. However, they are not in the same reference any more. Therefore, the discontinuity in the scan with the biggest amplitude for a given propagation mode would be considered as a reference for the incoming comparison and the same process applies to PAUT. The relative reference is then converted to a decibel value in order to correlate the flaw orientation directly with the suitable ultrasonic technique. The following section is highlighting the influence of the flaw orientation towards the chosen propagation mode algorithm.

4.3 Amplitude Consistency Towards Flaw Orientation

Table 3 and Table 4 present the amplitude of the 5 defects inside the test sample for each propagation modes (TT, TTT, TT-TT) and PAUT. An automatic tool has been used to extract the maximum amplitude value for each flaw. The green boxes represent the flaw having the maximum amplitude response of the recorded weld for a given mode. The green flaw was used as a reference when it came to the decibel difference value computation towards the other flaw.

Table 2 – Amplitude analysis of the acquisition of the left side of the weld

Mode	Acquisition of the left side of the weld									
	Flaw A Lack of fusion		**Flaw B Crack**		**Flaw C Porosities**		**Flaw D Porosities**		**Flaw E Lack of fusion**	
	Amplitude (%)	dB diff.	Amplitude (%)	dB diff.	Amplitude (%)	dB diff.	Amplitude (%)	dB diff.	Amplitude (%)	dB diff.
PAUT	100.8	-6.0	177.8	-1.0	102.0	-5.8	112.0	-5.0	200.0	0.0
TT	100.0	0.0	47.0	-6.6	80.6	-1.9	84.9	-1.4	67.4	-3.4
TTT	100.0	0.0	10.0	-20.0	85.7	-1.3	21.5	-13.4	27.4	-11.2
TT-TT	60.4	-4.4	84.9	-1.4	68.1	-3.3	39.7	-8.0	100.0	0.0

The left ultrasonic acquisition included all the discontinuities detected in the weld sample. The PAUT detected all the defects within 6 dB difference compared to the reference level. All the individual TFM modes exceeded this decibel difference for at least one defect compared to the reference level. As for example for the TTT mode, the crack with an amplitude of 10% have approximately 20 dB difference and at this level the flaw is considered undetected. Another example is the TT-TT mode, where the porosity has 8 dB difference compared to the mode reference. In such cases the flaw could easily be left undetected.

Table 3 – Amplitude analysis of the acquisition of the right side of the weld

Mode	Acquisition of the right side of the weld									
	Flaw A Lack of fusion		**Flaw B Crack**		**Flaw C Porosities**		**Flaw D Porosities**		**Flaw E Lack of fusion**	
	Amplitude (%)	dB diff.	Amplitude (%)	dB diff.	Amplitude (%)	dB diff.	Amplitude (%)	dB diff.	Amplitude (%)	dB diff
PAUT	---	---	---	---	97.1	-4.4	83.3	-5.8	161.9	0.0
TT	---	---	---	---	34.1	-9.3	100.0	0,0	76.4	-2.3
TTT	---	---	---	---	45.1	-6.9	31.7	-10.0	100.0	0.0
TT-TT	---	---	---	---	9.1	-20.8	9.9	-20.1	100.0	0.0

For the right side, only three flaws were detectable. For the TT-TT propagation mode, the lack of fusion has a strong amplitude compared to other flaws. This is due to the sensitivity of this method to lack of fusion orientation inside the test piece. Such specific behaviour emphasises the importance of selecting the appropriate reflector reference type and orientation prior to inspecting a weld with only one propagation mode.

Table 4 shows the average decibel variants compared to the reference, according to a given mode or technique. Such variations for the individual propagation mode usually occurs when the propagation mode and the flaw orientations are not compatible with each other. This table highlight the fact that PAUT acquisition technique is less sensitive to defect orientations compared to individual propagation modes such as TFM technique.

Table 4 – Means of the decibel deviation for left and right acquisitions

Mode	Mean dB deviation
PA	-4.78
TT	-4.58
TTT	-9.96
TT-TT	-12.37

Moreover, Table 4 highlights the unlikeliness of qualifying a weld qualification sample, based on ASME section V, Article IV, Mandatory Appendix IX when using only one propagation mode (3). Indeed, according to this standard, in order to qualify a test piece a notch is required on every bevel as well as a minimum of one vertical surface notch.

5 Conclusion

This paper identifies and compares a combination of techniques for weld inspection by based on the approach proposes in the thesis of Ms Kombossé. This was achieved by utilising the simulation results in an experimental setup, based on a real FMC/TFM acquisition testing a physical weld sample with verified defects. Moreover, the PAUT and TFM comparisons support the fact that efficient resolution and flaw sizing are achieved better utilising the TFM approach compared to the PAUT technique with the appropriate propagation mode.

The sensitivity towards to the flaw orientation indicates the possible amplitude variations for different propagation modes. In some application scenarios for a given combination of TFM modes on a defined flaw orientation, the decibel difference could reach up to 20 dB. Considering such amplitude change, it is doubtful that a single propagation mode could validate the integrity of a weld qualification sample. Therefore, utilising all three TFM propagation modes would improve the resolution and sizing capabilities of the inspection and minimising the risk of negligent due to defect orientations.

References

1. **Sy, Kombossé.** *Étude du développement de méthodes de caractérisation de défauts basée sur les reconstructions ultrasonores TFM.* Paris : Université Paris-Saclay, 2018.

2. **Association technique de traitement thermique.** *Métalographie et techniques d'analyse.* Paris : Dunod, 2004.

3. **American Society of Mechanical Engineers.** Section V, Article IV, Mandatory Appendix IX.